Encapsulation of Bacterial Spores in Nanoorganized Polyelectrolyte Shells

ARTICLE *in* LANGMUIR · JUNE 2009

Impact Factor: 4.46 · DOI: 10.1021/la900971h · Source: PubMed

Langmuir
Article
pubs.acs.org/Langmuir

Encapsulation of Bacterial Spores in Nanoorganized Polyelectrolyte Shells†

Shantanu S. Balkundi,‡ Nalinkanth G. Veerabadran,‡ D. Matthew Eby,§ Glenn R. Johnson,§ and Yuri M. Lvov*,‡

‡Institute for Micromanufacturing and Biomedical Engineering Program, Louisiana Tech University, Ruston, Louisiana, and §Microbiology and Applied Biochemistry, Air Force Research Laboratory - RXQL, Tyndall AFB, Florida

Received March 19, 2009. Revised Manuscript Received April 29, 2009

Layer-by-layer assembly uses alternating charged layers of polyionic polymers to coat materials sequentially in a sheath of functionalized nanofilms. Bacterial spores were encapsulated in organized ultrathin shells using layer-by-layer assembly in order to assess the biomaterial as a suitable core and determine the physiological effects of the coating. The shells were constructed on *Bacillus subtilis* spores using biocompatible polymers polyglutamic acid, polylysine, albumin, lysozyme, gelatin A, protamine sulfate, and chondroitin sulfate. The assembly process was monitored by measuring the electrical surface potential (ζ-potential) of the particles at each stage of assembly. Fluorescent laser confocal microscopy and scanning electron microscopy confirmed the formation of uniform coatings on the spores. The coating surface charge and thickness (20−100 nm) could be selectively tuned by using appropriate polymers and the number of bilayers assembled. The effect of each coating type on germination was assessed and compared to native spores. The coated spores were viable, but the kinetics and extent of germination were changed from control spores in all instances. The results and insight gained from the experiments may be used to design various bioinspired systems. The spores can be made dormant for a desired amount of time using the LbL encapsulation technique and can be made active when appropriate.

Introduction

The modification of the surface architecture of biological cells while retaining the internal working properties of the native system is a great challenge. Directly using or mimicking the processes of a biological cell in miniaturized devices will revolutionize system design; however, synthesizing the intricacies of biology is problematic.[1] To make such a modification, one has to work on the submicrometer scale and use benign reaction conditions that do not denature the properties of the biological materials. Cells require functional organic/inorganic interfaces, special fluidic support, and nutrition delivery. Moreover, the final 3D architectures must provide a compatible construction that does not disturb crucial elements of the cells.[2] Previous work explored the immobilization of mammalian cells in silica pores using chemical vapor deposition methods. The sol−gel matrices incorporate the cells within a scaffold intended to control multicellular organization; the approach may allow material to circumvent host immune reactions and support cell proliferation for tissue regeneration, but none of the approaches provided a bio/nanointerface for the 3D spatial control of biological cells.[3] Rubner et al. have fabricated polyelectrolyte multilayer patches on cells and have explored the surface functionalization of living cells. This technique is related to their earlier "Janus" technology of the asymmetrical functionalization of microparticles.[4−6] The modification of bacteria or bacterial spores brings additional challenges because they are much smaller (typically ca. 1 μm) and have a more fluid cell wall. The starting point of the current research was to reproduce some of the spore shell features using in vitro self-assembly methods.

Shell formation was based on layer-by-layer electrostatic assembly via the alternate adsorption of cationic and anionic species.[7−12] This mild nanoassembly method does not involve any covalent binding and is based on the cooperative electrostatic attraction of sequentially adsorbed polycations and polyanions. Every deposited polymer bilayer gives an approximately 2−5 nm thickness increment. Multilayers of four to five polyelectrolyte bilayers are permeable to low-molecular-weight molecules but cannot be penetrated by large macromolecules and proteins. Nanoorganized polyelectrolyte shells have already found applications in drug microencapsulation as a result of the tunable properties of the polyelectrolyte coatings.[13,14] Different numbers of polyelectrolyte layers in the shells and their different compositions have allowed the controlled release of drugs from such LbL capsules.[14] Researchers have successfully extended an LbL approach to 3D microparticles. Therefore, nutrition can be delivered to the cell in a controllable manner though the polyelectrolyte shells, and additional protection of the cell interior may be

† Part of the "Langmuir 25th Year: Self-assembled polyelectrolyte multilayers: structure and function" special issue.

*Corresponding author. E-mail: ylov@latech.edu.

(1) Baca, H.; Ashley, C.; Carnes, E.; Lopez, D.; Flemming, J.; Dunphy, D.; Singh, S.; Lopez, G.; Brozik, S.; Werner-Washburne, M.; Brinker, J. *Science* **2006**, *313*, 337–340.
(2) Zhang, S. *Nat. Biotechnol.* **2004**, *22*, 151–155.
(3) Stevens, M. *Science* **2005**, *310*, 1135–1139.
(4) Swiston, A.; Cheng, C.; Um, S.; Irvine, D.; Cohen, R.; Rubner, M. *Nano Lett.* **2008**, *8*, 4446–4453.
(5) Yang, S.; Lee, D.; Cohen, R.; Rubner, M. *Langmuir* **2004**, *20*, 5978–5981.
(6) Li, Z.; Lee, D.; Rubner, M.; Cohen, R. *Macromolecules* **2005**, *38*, 7876–7879.
(7) Lvov, Y.; Ariga, K.; Ichinose, I.; Kunitake, T. *J. Am. Chem. Soc.* **1995**, *117*, 6117–6123.
(8) Decher, G. *Science* **1997**, *277*, 1232–1237.
(9) Shutava, T.; Kommireddy, D.; Lvov, Y. *J. Am. Chem. Soc.* **2006**, *128*, 9926–9934.
(10) Donath, E.; Sukhorukov, G.; Caruso, F.; Davis, S.; Möhwald, H. *Angew. Chem., Int. Ed.* **1998**, *6*, 413–418.
(11) Caruso, F.; Caruso, R.; Möhwald, H. *Science* **1998**, *282*, 1111–1114.
(12) Shenoy, D.; Antipov, A.; Sukhorukov, G.; Möhwald, H. *Biomacromolecules* **2003**, *4*, 265–272.
(13) Richert, L.; Lavalle, P.; Vautier, D.; Senger, B.; Stolz, J.; Schaaf, P.; Voegel, J.; Picart, C. *Biomacromolecules* **2002**, *6*, 1170–1178.
(14) Ai, H.; Jones, S.; DeVilliers, M.; Lvov, Y. *J. Controlled Release* **2003**, *86*, 59–66.

provided. Furthermore, the polyelectrolyte coating may protect cells from immune attacks, protect them under harsh conditions, and even decompose external harmful agents through active border defense, as was demonstrated in ref 9 for catalase-assisted hydrogen peroxide decomposition in LbL multilayers. The modification of whole cells can guide them to selected tissues or organs as was demonstrated for the targeting of platelets containing an antibody within the outer layer of the deposited LbL shell.[15]

We and other groups have used this technique to encapsulate blood cells (erythrocytes and platelets), yeast cells, and mesenchymal stem cells.[15−21] Synthetic polyelectrolytes, anionic sodium poly(styrene sulfonate), and cationic poly(allylamine) hydrochloride were used to form nanoorganized shells on single cells. The shell formation was confirmed with fluorescent laser confocal microscopy, AFM, and small-angle neutron scattering. LbL assembly of natural polyelectrolytes (chitosan, alginate, and hyaluronic acid) also allowed the encapsulation of *Escherichia coli* cells, and experiments using a second generation of *E. coli* cells demonstrated that cell activity was sustained in the presence of the polyelectrolyte shell.[19] The same LbL technology allowed the introduction of enzymatic activity onto yeast cell shells in order to promote the conversion of lactate into pyruvate.[20] If one can modify bacterial pathogenesis as a means of delivery, then it may also have future applications in drug and gene delivery.

Although researchers have tried various encapsulation techniques for bacteria (spray drying, extrusion, emulsion, and phase separation), not much has been done in the field on spore encapsulation to explore the temporal and spatial control of spore germination. In the present work, we demonstrate the engineered coating of bacterial spores with thin multilayers of various polyelectrolytes, proteins, and nanoparticles using layer-by-layer deposition. Following assembly, the coat morphology was characterized using fluorescent laser confocal microscopy and scanning electron microscopy. Spore viability and germination kinetics were monitored by quantifying the release of dipicolinic acid, which occurs at the onset of spore germination.

Experimental Section

Reagents and Materials. *Bacillus subtilis* strain 168 was obtained from the American-type culture collection (ATCC 23857). Synthetic sodium poly(styrene sulfonate) (PSS, M_w = 100 kDa), poly(dimethyldiallyl ammonium chloride) (PDDA, M_w = 100 kDa), biocompatible polyelectrolytes polyglutamic acid (PGA, M_w = 50 kDa) and polylysine (PLL, M_w = 50 kDa), gelatin A, and proteins albumin and lysozyme were all obtained from Sigma-Aldrich. For fluorescent confocal microscopy measurements, rhodamine isothiocyanate (RITC)-labeled polyallylamine hydrochloride and polylysine were used. RITC was obtained from Sigma-Aldrich. Silica nanoparticles (Ludox TM-40 colloidal silica, 40 wt % suspension in water) were also obtained from Sigma-Aldrich. 2,6-Pyridine dicarboxylic acid (DPA, 99%) and terbium chloride hexahydrate ($TbCl_3$, 99.9%) were also purchased from Sigma-Aldrich. L-Alanine (L-Ala, ≥99.5%) was purchased from Fluka. All other reagents were purchased from Sigma-Aldrich and were of the highest purity available.

Spore Preparation and Isolation. *B. subtilis* was grown overnight in nutrient media and spread onto sporulation agar plates, as previously reported.[22] After the plates were incubated for 3−5 days at 37 °C, sterile water was added to each plate, and the cellular material was collected by scraping with a bent glass rod and decanting the slurry into a sterile centrifuge tube. The cell slurry was centrifuged at 15 000*g* for 10 min. The cells were lysed by resuspending a pellet in an equal volume of SDS solution (0.5%) and then centrifuged to collect spores (15 000*g*, 10 min); the supernatant containing cell debris was discarded. The spore pellet was suspended and collected two additional times using the SDS treatment and then five times with sterile water to remove trace amounts of SDS. The purity of the spore preparations was confirmed by microscopic inspection and the malachite green spore stain procedure.[23] Spores were resuspended in sterile water, transferred to glass ampules (10^8 to 10^9 spores ampule^{-1}), lyophilized, and sealed in the tubes when under vacuum. The samples were stored at −20 °C until use.

Shell LbL Assembly. All treatment and layering steps were done at 25° (except where noted), and the samples were contained in 1.5 mL polypropylene centrifuge tubes. The bacterial spore samples were resuspended in 1 mL of ultrapure water (DI) before use in the LbL assembly. The sample was then centrifuged at a speed of ∼ 9000 rpm, and the supernatant was replaced with pure water. The spore sample was washed three times to make sure that it was free of the medium. The cells were further suspended in 0.75 mL of water and were ready for assembly. The concentration of aqueous polyelectrolytes was 2 mg/mL (pH 6.8). All polymer samples were treated briefly in a sonicating bath and then vortex mixed before use in the assembly. Gelatin A solution was heated to 45 °C for 5 min prior to the layering steps. Polyelectrolytes (0.5 mL) were added to 0.75 mL of the spore dispersion and held for 15 min for adsorption completion. Polycations and polyanions were adsorbed sequentially and washed with 1 mL of DI water between steps, and spore separation from supernatants was achieved via centrifugation. The spore samples were briefly sonicated after each washing step to prevent aggregation. Conditions of the polycation /polyanion sequential adsorption and bilayer thickness optimization were elaborated using a QCM instrument (quartz crystal microbalance, 9 MHz, silver-plated electrodes of 0.16 cm^2, USI-System Co, Japan). We used the Saurbrey's equation-based formula L (nm) = $-0.017\Delta F$ (Hz) to determine the thickness of the films (L) with the coefficient based on SEM scaling of one of the samples as described in ref 7.

Zeta Potentiometer Measurements. An electrical surface ζ potential of the bacterial spores and of the polyelectrolytes shells on the spores was measured using a ZetaPlus potential analyzer (Brookhaven ZetaPlus microelectrophoretic instrument); six measurements for each sample were made to ensure data reliability.

Confocal Microscopy. Encapsulated bacterial spores were coated with a final layer of cationic polymer labeled with rhodamine isothiocyanate (RITC). The samples were then washed three times by centrifuging and resuspending the cells in ultrapure water. Ten microliters of the sample was sufficient to visualize the capsules under the Leica DMI RE2 confocal laser scanning microscope. A 63× oil immersion objective lens was used to image the encapsulated cells.

Scanning Electron Microscopy. A Hitachi S 4800 FE scanning microscope was used to image uncoated and encapsulated spores. To enhance image clarity, preformed silica nanoparticles were coated onto the spore shell surface prior to SEM analysis. The positive surface charge on the PAH-encapsulated spores allowed a reasonably strong ionic interaction with silica. Silica nanoparticles (22 and 72 nm diameters) were diluted in water (final concentration 1 mg/mL). The silica nanoparticle dispersion

(15) Hua, A.; Fang, M.; Jones, S.; Lvov, Y. *Biomacromolecules* **2002**, *3*, 560–564.
(16) Neu, B.; Voigt, A.; Mitlohner, R.; Leporatti, S.; Gao, C.; Donath, E.; Kiesewetter, H.; Möhwald, H.; Meiselman, H.; Bäumler, H. *J. Microencapsulation* **2001**, *18*, 385–395.
(17) Diaspro, A.; Silvano, D.; Krol, S.; Cavalleri, O.; Gliozzi, A. *Langmuir* **2002**, *18*, 5047–5050.
(18) Yu, M.; Ivanisevic, A. *Biomaterials* **2004**, *25*, 3655–3662.
(19) Estrela-Lopis, I.; Leporatti, S.; Typlt, E.; Clemens, D.; Donath, E. *Langmuir* **2007**, *23*, 7209–7215.
(20) Hillberg, A.; Tabrizian, M. *Biomacromolecules* **2006**, *7*, 2742–2750.
(21) Veerabadran, N.; Stewart, S.; Lvov, Y.; Mills, D *Macromol. Biosci.* **2007**, *37*, 877–882.
(22) Schaeffer, P.; Millet, J.; Aubert, J.-P. *Proc. Natl. Acad. Sci. U.S.A.* **1965**, *54*, 704–709.
(23) Schaeffer, A.; Fulton, M. *Science* **1933**, *77*, 194–198.

Scheme 1

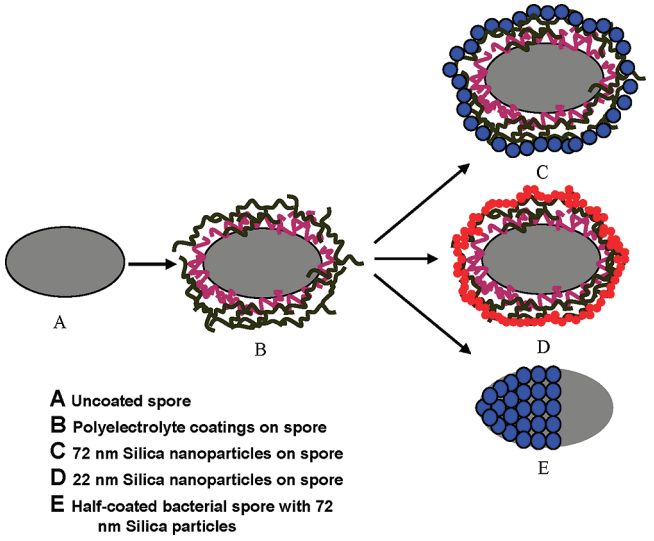

(0.5 mL) was added to ~0.1 mL of a PAH−RITC-labeled encapsulated bacterial spore solution and incubated for 30 min for adsorption completion. The sample was then rinsed with water and centrifuged at 9000 rpm to remove the excess silica. Finally, the sample was suspended in 1 mL of water, and 0.1 mL of this sample was used for SEM studies. The sample was allowed to air dry and was not heated while an iridium layer was deposited via sputtering (3 nm thickness).

Spore Germination Kinetic Assays. Spore viability was measured using a spore germination assay, as previously described.[24] The assay is based upon dipicolinic acid (DPA) release following germination induction by L-alanine exposure. DPA release is monitored over time by measuring the fluorescence emission of DPA when bound to terbium ions. Spore preparations were resuspended in ultrapure water to final concentrations on the order of 10^6 and 10^8 viable spores mL^{-1}. Viable spore counts were measured by plating serial dilutions of the spore preparations onto solid nutrient media and enumerating colonies. Spore preparations and serial dilutions were vigorously vortex mixed before plating to disrupt aggregated spores. To activate spores before germination, spore preparations were incubated at 70 °C for 30 min. After incubation, spore solutions were diluted 1:10 in germination buffer (1.1 mM L-alanine, 10 μM $TbCl_3$, 0.45% NaCl, 0.25 mM sodium acetate, pH 5.6) and incubated in a microtiter plate at 37 °C. DPA release during germination was monitored in situ by measuring the Tb−DPA emission spectrum over time in the microtiter plate. %DPA released is calculated by first measuring the basal level of DPA in spore preparations and also the total DPA content in spores. To measure the total DPA content in spore suspensions (100% DPA release), the original spore preparation was diluted 1:10 in 0.653 mM dodecylamine and incubated at 60 °C for 10 min to extract the available DPA.[25] After extraction, the spore solution was diluted 1:10 in germination buffer and immediately measured to determine the concentration of the Tb−DPA complex. The basal level of the DPA in spore preparations (0% DPA release) was found by treating the activated spore solutions as described above except that the germinant, L-alanine, was omitted. For each assay measurement, the relative fluorescence intensity was normalized to the fluorescence intensity of the buffer solution without spores and then to the basal DPA concentration and total DPA in spore preparations according to $(F_x - F_{0\%})/(F_{100\%} - F_{0\%})$, where F_x is the fluorescence intensity of the sample, $F_{100\%}$ is the fluorescence from the total amount of DPA in the spore preparation, and $F_{0\%}$ is the fluorescence intensity of the basal DPA concentration. Each germination assay was completed in triplicate for native spores and each layering method.

(24) Hindle, A.; Hall, A. *Analyst* **1999**, *124*, 1599–1605.
(25) Pelegrino, P. M.; Fell, N. F.; Gillespie, J. B. *Anal. Chim. Acta* **2002**, *455*, 167–172.

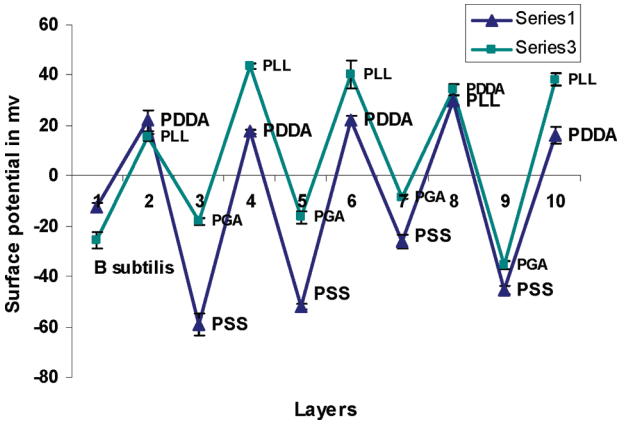

Figure 1. ζ-potential of a *B. subtilis* spore in DI water at pH 6.8, showing alternation with successive deposition of cationic and anionic polyelectrolytes (synthetic: poly(dimethyldiallyl ammonium chloride), PDDA; sodium poly(styrene sulfonate), PSS; poly(lysine), PLL; and poly(glutamic acid), PGA).

Fluorimetry. Fluorometric analysis was completed using a microplate-compatible fluorometer (Synergy HT) with time-resolved fluorescence capability and Gen5 version 1.02.8 software (BioTek Instruments Inc., Winooski, VT). Samples were analyzed in UV-transparent plastic 96-well microtiter plates from Corning Inc. (product no. 3635, Acton, MA). The excitation wavelength was 275 nm, and the emission wavelength was 545 nm with bandwidths of 10 and 40 nm, respectively. The optics were positioned to read from the bottom of the microtiter plate, and the sensitivity was set at 180. The time delay before reading after excitation was 0.1 ms, the duration of the reading was 9.9 ms, and 10 reads were completed per well.

Results and Discussion

The ζ-potential measurements indicated that the surface potential of washed *B. subtilis* spores is −22 ± 2 mV (Figure 1). Therefore, the LbL assembly processes were started with the adsorption of cationic polymers. The adsorption of positively charged PDDA converted the spore surface charge to modestly positive polarity. The first shell assembly process proceeded with the alternate adsorption of synthetic PDDA and PSS, which resulted in symmetric changes in the spore potential to positive and negative, characteristic of the LbL process. After the deposition of four bilayers of PDDA/PSS, the ζ potential was −50 mV after the PSS adsorption step and +20 mV at the final PDDA coat (10th step in Figure 1). Therefore, the treatment can strongly influence the spore surface charge, reversing the polarity to strongly positive or greatly enhancing the negative charge compared to that of the initial noncoated spores. The outermost PSS was more negatively charged than the outermost PDDA, but this tendency was changed for polyglutamic acid (PGA) alternated with polylysine (PLL). The PDDA/PSS-encapsulated spores could be stably dispersed in aqueous solvents and did not aggregate because of the strong surface charge. One can stop the assembly on polyanion adsorption stage to have spores with negative surface charge or add one more polycation layer to have outermost positive spores.

At the next stage of the work, we used the biocompatible polyelectrolytes poly(lysine) (PLL) and poly(glutamic acid) (PGA) as the coating substrates. PLL is positively charged and PGA is negatively charged at pH 6.5−7 due to amine and acid ionized

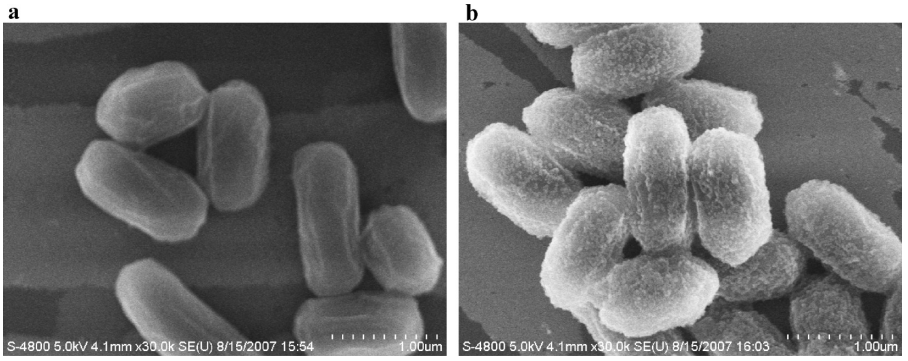

Figure 2. SEM images of *B. subtilis* spores (control shown in panel a) and of *B. subtilis* coated with (PLL/PGA)4 + PLL + 22 nm silica nanoparticles (b).

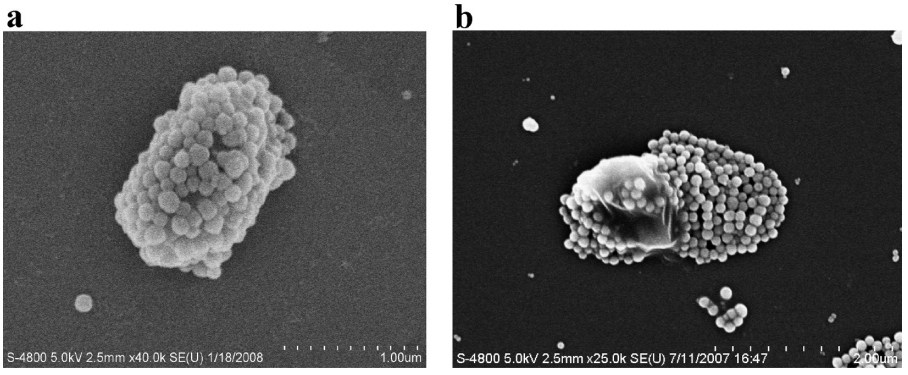

Figure 3. SEM images of *B. subtilis* spores coated with $(PLL/PGA)_4$ + PLL + 72 nm silica nanoparticles (two different spores).

groups, correspondingly. Again, deposition of the first layer of polylysine led to a positive ζ-potential (+16 mV). Deposition of the following anionic PGA layer decreased the ζ-potential to −18 mV. The subsequent layer-by-layer PDDA/PGA deposition steps enhanced the surface ζ-potential and showed an almost reproducible electrical potential reversal between +45 mV after PLL adsorption to −35 mV for PGA adsorption after four bilayer shell formation (Figure 1).

The QCM measurements assumed a difference in the thickness of deposited polyelectrolyte multilayers. The assembly of PSS/PDDA multilayer provided an increment of 2.2 ± 0.2 nm for each bilayer, and the PLL/PGA multilayer processes showed 3.5 ± 0.4 nm for each bilayer when in a dry state. QCM assembly monitoring was performed on the model QCM electrode surface, and results were transferred to the spore shell thickness as an estimation, not taking into account the specificity of the spore surface. In the hydrated state, the thickness of the multilayer wall will be 2 times larger.[7,12] Accordingly, the thickness of the $(PLL/PGA)_4$ shell may be estimated as 28 ± 5 nm.

The surfaces of the LbL-coated spores were decorated with nanomaterials of known composition and size in order to image surface topology because conventional staining methods will not selectively modify the polyelectrolyte layers compared to the spore coat. We obtained spores that were evenly coated with the nanoparticles, providing them with an inert, mechanically stable layer. This also helped us in studying the changes in the surface architectures. Negatively charged silica nanoparticles were deposited on the outermost shell (after polycations) and provided visualization using scanning electron microscopy. The ζ-potential of the $(PLL/PGA)_4$-modified spores that were subsequently coated with + PLL/silica decreased to −30 mV because of the adsorption of the negative outermost silica layer (not shown in Figure 1). After careful washing, the samples were studied under a scanning electron microscope and compared to uncoated spores (Figure 2). It appears that a layer of the 22-nm-diameter silica particles adsorbed on the entire cell surface of the polycation-treated spores to provide a uniform coating. The formation of the shell with larger 72-nm-diameter silica was also possible as demonstrated in Figure 3a, but together with well-coated spores, some of the spores came out "half-dressed". Surveys of the multiple fields during SEM analysis revealed that 10−15% of the treated spores were coated with 72 nm silica spheres. The incomplete nanoparticle coating may be related to surface properties of certain parts of the coated spore surface. The differences may result when repulsive forces between the larger silica nanospheres are stronger than attraction by the PLL coating, or possibly some of the surface poorly adsorbed the polymer and led to part of the layer breaking off of the surface.

Fluorescence confocal microscopy using rhodamine isothiocyanate (RITC)-labeled PLL is presented in Figure 4. In initial experiments, we found evidence that the RITC could penetrate the spore coats that were modified with four bilayers of PLL-PGA. The result may suggest that the preceding LbL process was somehow imperfect and that the PLL-RITC crossed the previous synthetic bilayers and then breeched the spore surface. An alternative explanation would be that noncovalently bound RITC is released from the layer and penetrates the spore surface.

This phenomenon was overcome in subsequent modification of the synthetic shell composition. The addition of a penultimate layer of gelatin A blocked the dye from crossing the synthetic coating or spore coat. The green autofluorescence from the spore interior is evident with images using a 530 nm filter; an identical response is found with unlabeled spores under confocal imaging (not shown). Subsequent fluorescent images in transmission mode show that the all of the spores present in the field are coated with the shell containing the RITC. A well-defined red layer evenly

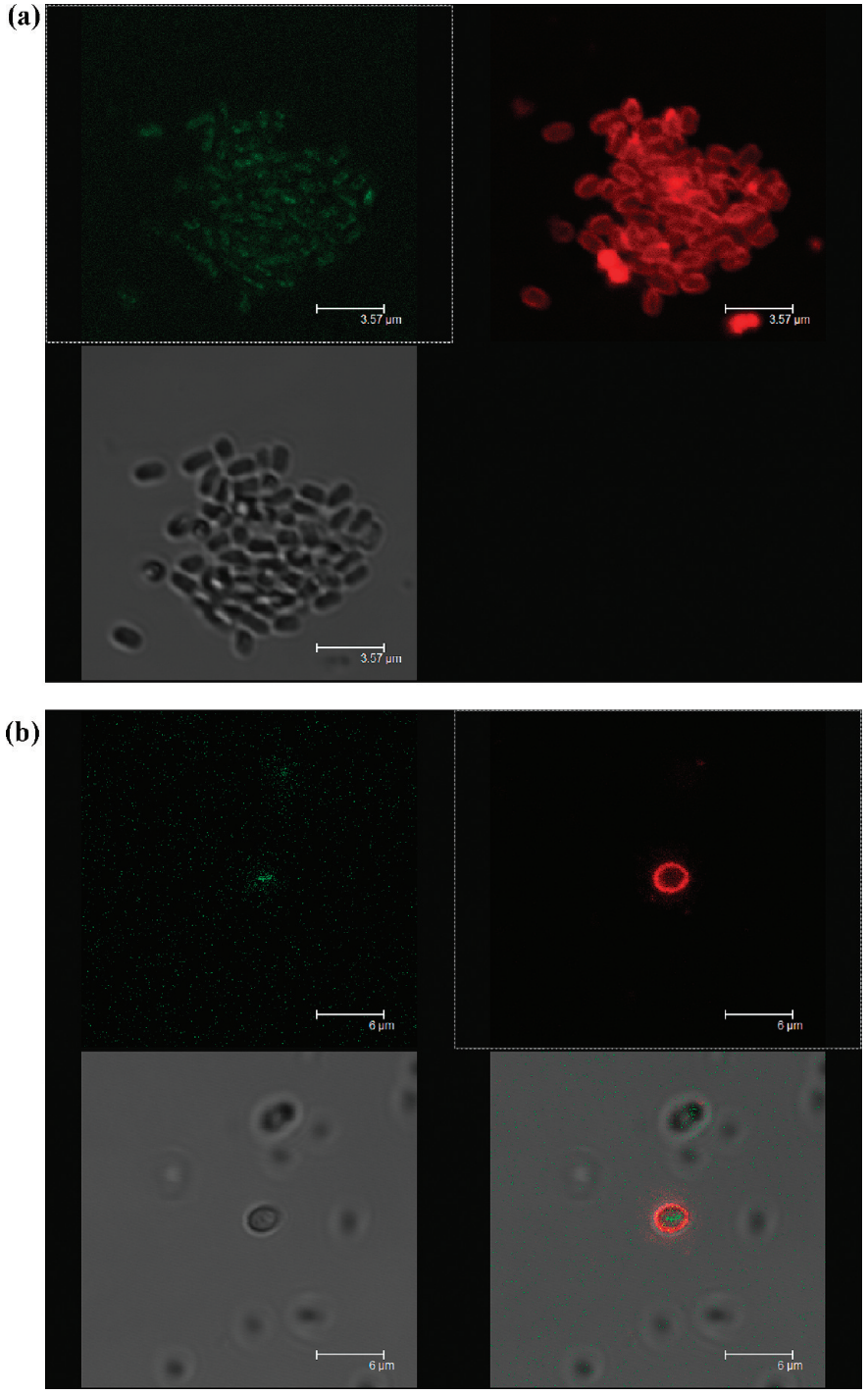

Figure 4. (a) Confocal image of *B. subtilis* with a shell of $(PLL/PGA)_4$ labeled with PLL-RITC, immediately after the shell assembly (1st day). (b) Confocal image of *B. subtilis* with a shell of $(PLL/PGA)_4$−gelatin labeled with PLL-RITC (15th day).

coated the spore surface, indicating that the structural morphology of the spore was retained (Figure 4a,b). The image does not represent an actual polyelectrolyte shell wall because the limit for confocal microscope resolution is approximately 200 nm whereas the actual shell thickness is likely no greater than 30 nm. The LbL shell provided a robust surface coating, and after 15 days of storage at 4 °C, the shell remained intact on the nongerminated spore surfaces (Figure 4b).

Effect of Coatings on Spore Viability and Germination. Measurements of spore germination using the DPA release assay distinguish the rate and extent of germination of the various spore preparations. In all cases, the spores retained viability; this was clear in simple cultivation showing that vegetative cells grew out from spore inoculum and was clearly evident in DPA assay results. The assay measured the apparent germination kinetics and variation in the onset of germination within the population. Following the addition of a soluble germinant, the fluorescent DPA−terbium complex was detected almost immediately, showing insignificant differences in the onset of germination compared to the uncoated controls (Figure 5). The result suggests that the synthetic layers were permeated by the germinant; however, the initial rate of DPA release differed. As one would expect, the coating reduces coat permeability, which was reflected by a reduced rate of initial DPA release. The extent of DPA release

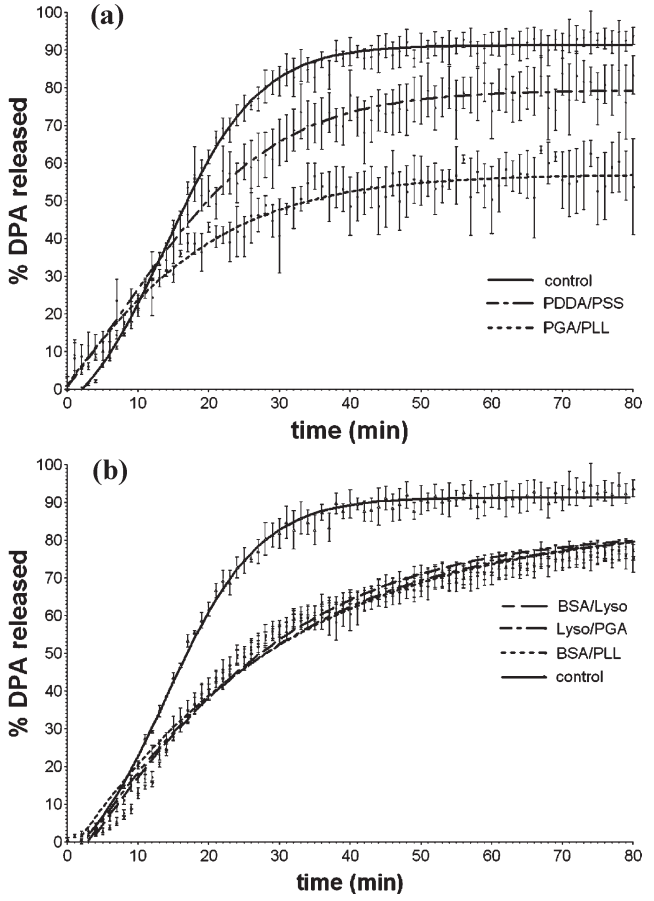

Figure 5. (a, b) Kinetics of apparent spore germination monitored by th erelease of dipicolinic acid (DPA). Data for control spores and spores coated with different shell compositions (four bilayers with alternate polycation and polyanions) are indicated. Test samples were normalized to yield equivalent colony-forming units per milliliter of sample.

differed among the modified spores compared to the controls. The cells coated with PGA/PLL bilayers showed the greatest effect with only 50% apparent germination compared to the potential in the sample. All other shells reached a plateau of about 70% of the chemically lysed samples. The controls showed approximately 90% germination using the present time scale and treatment. The difference in total DPA release compared to the control may be due to a portion of spores that are present but unable to germinate normally during assay.

Conclusions

Bacterial spores are effectively encapsulated using layer-by-layer polyelectrolyte assembly methods. Individual bacterial spores were coated using synthetic and natural polyelectrolytes to form coatings as thick as 30 nm on the surface of the spores with a surface ζ potential that could be adjusted between -30 and $+40$ mV. It was possible to refine the coated structure further with a finishing layer composed of silica nanoparticles. The finishing process adds to the toolbox available for nanoscale precision coatings and may impart further mechanical stability to the engineered architectures. Germination assays show that the spores are viable even after encapsulation using various polyelectrolytes. The coatings appear to affect the diffusion rates of germinant influx into and possibly actual endospore germination. Customizing the coatings to control germination rates could be useful in specifically coordinating germination. For example, the number of layers or type of polymer might be adjusted to further affect the response to usual germinants. The effectiveness of the bioderived polymers is also notable. The materials (simple amino acid-based polymers and proteins) may be more environmentally compatible and thus amenable to open applications such as agricultural biopesticides.

Acknowledgment. S.S.B. was supported through a predoctoral fellowship administered by the Oak Ridge Institute of Science and Engineering. Work at Tyndall AFB was supported by funding from the Air Force Office of Scientific Research (J. Gresham, Program Manager) and the Air Force Research Laboratory Materials Science Directorate. This work was also supported by NSF-EPSCoR no. 34768. Any opinions, findings, and conclusions or recommendations expressed in this material are those of the authors and do not necessarily reflect the view of the National Science Foundation.